

ORIGINAL ARTICLE

Δ Np63 α promotes adhesion of metastatic prostate cancer cells to the bone through regulation of CD82

V Di Giacomo^{1,2,6}, TV Tian^{1,2}, A Mas^{1,2}, M Pecoraro^{1,2,7}, L Batlle-Morera^{1,2}, L Noya³, J Martín-Caballero⁴, J Ruberte³ and WM Keyes^{1,2,5}

Δ Np63 α is a critical mediator of epithelial development and stem cell function in a variety of tissues including the skin and breast, while overexpression of Δ Np63 α acts as an oncogene to drive tumor formation and cancer stem cell properties in squamous cell carcinoma. However, with regards to the prostate, while Δ Np63 α is expressed in the basal stem cells of the mature gland, during adenocarcinoma development, its expression is lost and its absence is used to clinically diagnose the malignant state. Surprisingly, here we identify a sub-population of bone metastatic prostate cancer cells in the PC3 cell line that express Δ Np63 α . Interestingly, we discovered that Δ Np63 α favors adhesion and stem-like growth of these cells in the bone microenvironment. In addition, we show that these properties require expression of the target gene CD82. Together, this work uncovers a population of bone metastatic prostate cancer cells that express Δ Np63 α , and provides important information about the mechanisms of bone metastatic colonization. Finally, we identify metastasis-promoting properties for the tetraspanin family member CD82.

Oncogene (2017) 36, 4381–4392; doi:10.1038/onc.2017.42; published online 3 April 2017

INTRODUCTION

P63 is a member of the p53 family of transcription factors, and contains two main isoforms of the protein, designated transactivating and deltaN (Δ N). Further variability is given by alternative splicing, generating three main variants for each isoform (α , β and γ).¹ In general, the TAp63 isoforms function more similarly to p53 in regulating apoptosis and senescence, while Δ Np63 has been linked with stem cell fate and proliferation.^{2,3}

In tumor development, Δ Np63 α is overexpressed in the majority of human squamous cell carcinoma, and recent studies demonstrated an oncogenic role for this isoform during squamous cell carcinoma formation.^{4,5} With regards to prostate cancer (PC), however, there is a different expression pattern. P63 is detected in the basal stem cells of the normal tissue, and is suggested to identify the tumor-initiating population in mouse and human cancers.^{6,7} Subsequently the expression of Δ Np63 α is lost during the transformation process and growth of the primary prostate tumor. As such, PC is negative for Δ Np63 α , and assessment of p63 negativity is used clinically to diagnose tumor status.^{3,7–10}

With the aim of modeling metastatic PC, many studies have benefited from the use of three cell lines derived from individual metastatic sites, to investigate the cellular and molecular processes involved. These include PC3 cells, derived from bone metastasis, DU145 cells from brain and LNCaP from lymph node. Within these, only PC3 is capable of forming bone metastasis in mouse when the cells are introduced via intra-cardiac or intra-tibial injection. Interestingly, this cell line contains cancer stem-like cells that are more aggressive in forming tumors *in vivo*.^{11–13} In agreement with clinical data, all these cell lines have been described to be negative for p63 expression.

Unexpectedly we identified a sub-population of cells in the PC3 line that expresses Δ Np63 α . Through functional misexpression studies *in vivo*, coupled with detailed molecular profiling, we discovered that Δ Np63 α contributes to the adhesion and colonization of these bone metastatic PC cells. Interestingly, these cells have a shared signature with normal stem-like cells, and in particular, increased expression of the adhesion molecule CD82. Surprisingly, functional follow-up studies identified pro-metastatic functions for CD82, through the regulation of cell adhesion. Together, this identifies previously unknown heterogeneity in the PC3 bone metastatic cell line, and further supports how promotion of stem-like properties may favor metastatic growth.

RESULTS

Δ Np63 expression is enriched in the basal stem cells of the adult mouse prostate

Studies with p63-deficient models have demonstrated a requirement for p63 in the development of the prostate.^{14–16} In addition, p63 expression has been documented in basal cells in the adult gland that express stem cell markers.^{7,17} These observations suggest critical roles for p63 in adult prostate stem cells (PSC), yet the underlying mechanisms remain unknown. We validated previous studies demonstrating specific p63 expression in the small Keratin 5-positive basal cells of the prostate, and in close proximity to the Keratin 18 luminal cells, which are negative for p63 (Supplementary Figures 1A,B). Next, we dissociated the glands to a single cell suspension, and fluorescence-activated cell sorting (FACS) sorted the basal stem cell population using the previously characterized PSC markers CD49f and Sca-1.^{17,18} By performing RT-qPCR, we showed that Δ Np63 expression is highest in the double-positive CD49f/Sca-1

¹Gene Regulation, Stem Cells and Cancer Program, Centre for Genomic Regulation (CRG), The Barcelona Institute of Science and Technology, Barcelona, Spain; ²Universitat Pompeu Fabra (UPF), Barcelona, Spain; ³Department of Animal Health and Anatomy and Center for Animal Biotechnology and Gene Therapy, Universitat Autònoma de Barcelona, Barcelona, Spain; ⁴Unidad de Animal de Laboratorio, PRBB, Barcelona, Spain and ⁵Development and Stem Cells program, Institut de Génétique et de Biologie Moléculaire et Cellulaire, CNRS UMR7104, Inserm U964, Université de Strasbourg, Illkirch, France. Correspondence: Dr B Keyes, Centre for Genomic Regulation (CRG), The Barcelona Institute of Science and Technology, Carrer del Dr Aiguader, 88, 08003 Barcelona, Spain.

E-mail: bill.keyes@crg.eu

⁶Current address: ZeClinics, Barcelona, Spain.

⁷Current address: Department of Proteomics and Signal Transduction, Max Planck Institute of Biochemistry, Martinsried, Germany.

Received 29 July 2016; revised 1 January 2017; accepted 19 January 2017; published online 3 April 2017

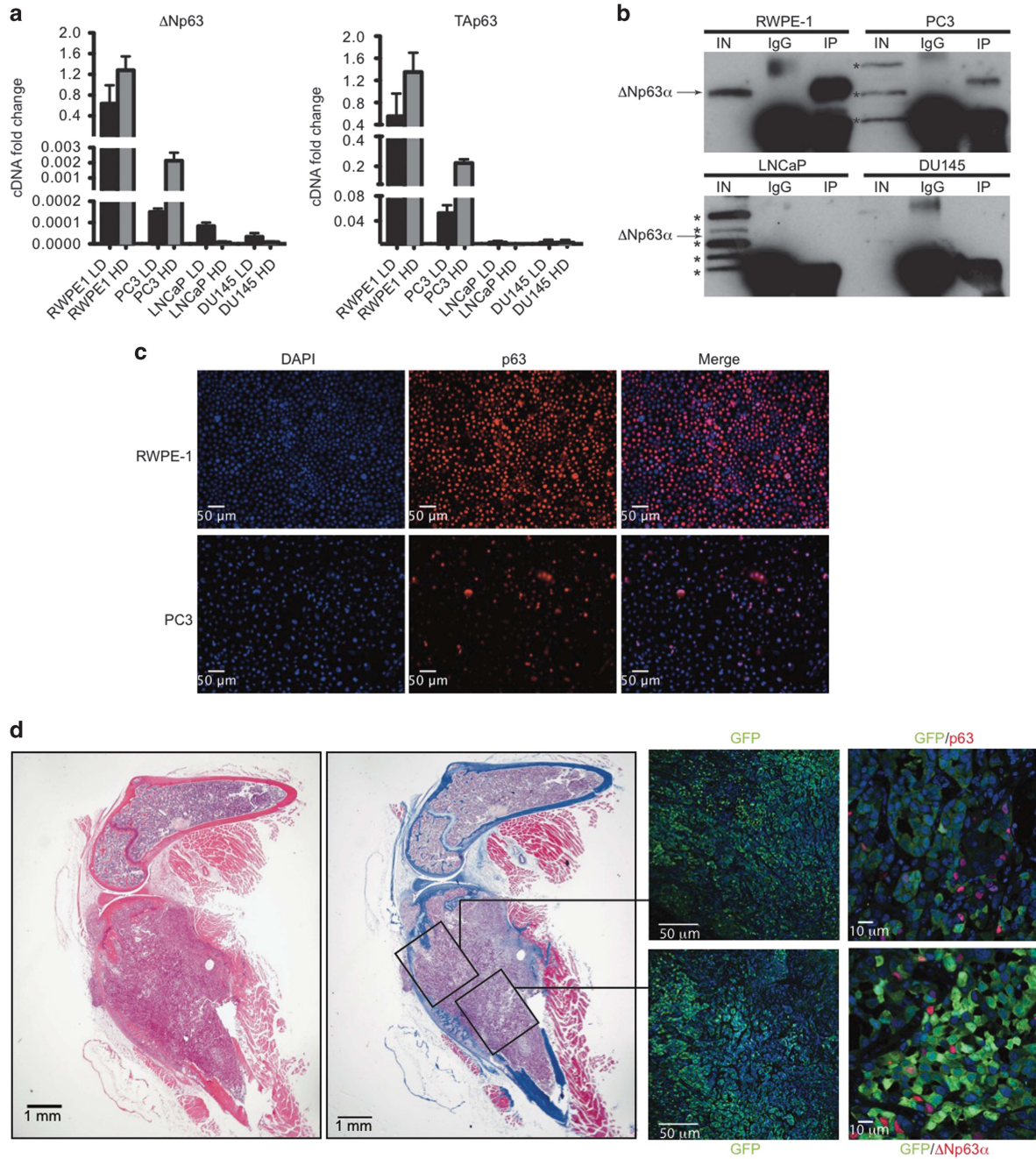


Figure 1. Δ Np63 α is expressed in a sub-population of PC3 human bone metastatic cells. **(a)** RT-qPCR for the Δ N and transactivating isoforms of p63 in four prostate cell lines: RWPE-1, PC3, LNCaP and DU145. Low density (60–70% confluency), LD; high density (100% confluent), HD. Values are compared to those of RWPE-1 LD replicate as reference. Graphs show results as mean \pm s.e.m. of three biological replicates. **(b)** IP and western blot for p63 in the four prostate cell lines. Input, IN; IP with immunoglobulin G control, IgG; IP with the p63-specific antibody, IP. Arrows denote the height where the Δ Np63 α band is expected and asterisks indicate unspecific bands in the LNCaP input lane that are not present in the IP lane. **(c)** Immunofluorescence for p63 on RWPE-1 and PC3 cells in culture. **(d)** PC3 cells were infected with a reporter-vector and injected intra-tibially in adult nude mice. The derived bone metastases were identified by immunohistochemical staining for GFP. P63 (and specifically Δ Np63 expression) was found in a sub-population of GFP+ metastatic cells in bone.

stem cells (Supplementary Figure 1C, D). We confirmed this at the protein level, performing cytospin-immunostaining on the same populations (Supplementary Figures 1E and F).

Δ Np63 α is expressed in a sub-population of human metastatic PC cells

Unlike the normal prostate gland, PC and PC cell lines are considered negative for p63 expression.^{8,10,19} Surprisingly

however, we detected expression of Δ Np63 in PC3 cells, an aggressive cancer cell line derived from metastasis to the bone. Indeed, very low levels of the Δ Np63 transcript was only detectable in this cell line, and not in others derived from prostate metastasis to the lymph node (LNCaP) and brain (DU145) (Figure 1a). Interestingly, the expression of the transcript increased in high-density cultures (100% confluency) compared to low density/exponential phase proliferating cells (60–70% confluency).

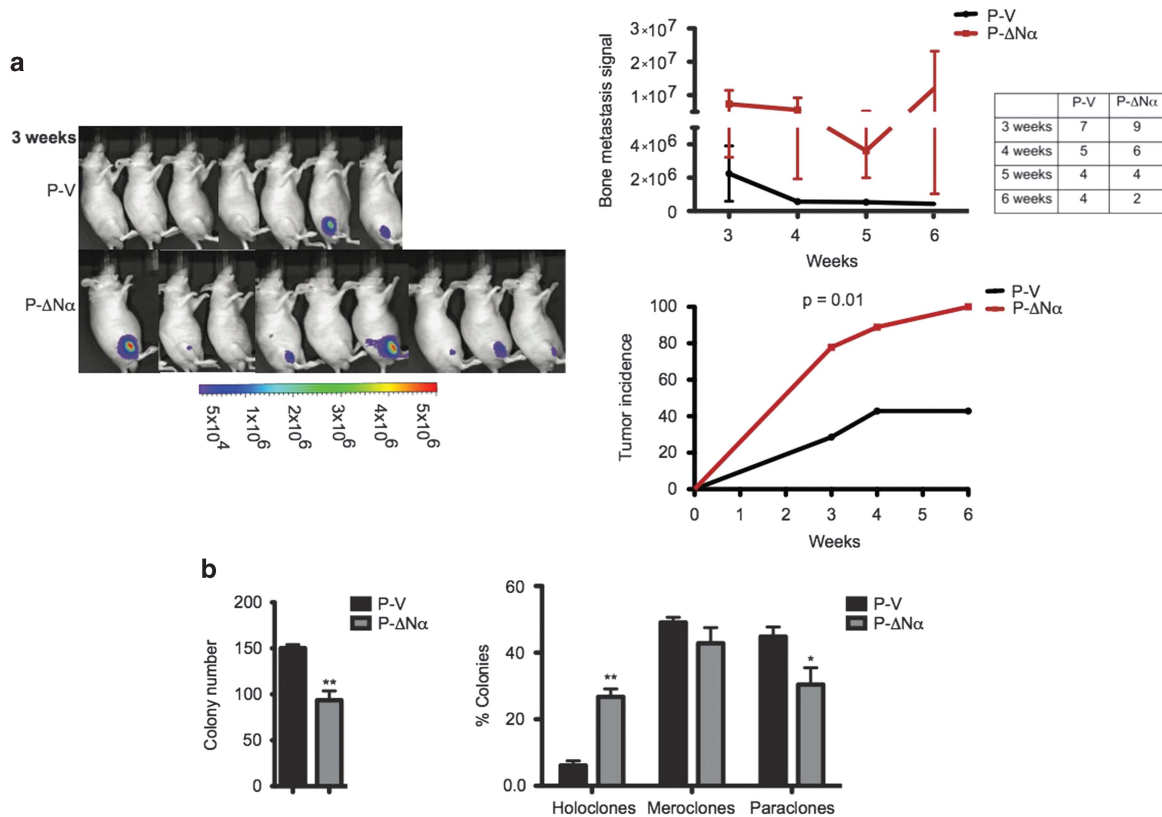


Figure 2. Δ Np63 α confers a growth advantage and stem-like properties to PC3 cells in the bone microenvironment. **(a)** Adult male nude mice were injected intra-tibially with 2.5×10^5 PC3 cells infected with vector control (P-V) or overexpressing Δ Np63 α (P- Δ N) and co-infected with the Luc-GFP construct. Bone metastasis was monitored weekly by luciferase imaging beginning from week 3. Seven mice were analyzed for the P-V group and nine for the P- Δ N α group. Animals were killed at different time points depending on the appearance of the tumor. The table indicates the total number of mice that were measured for a luciferase signal at each time point. Bone metastasis luciferase signal and tumor incidence are represented as previously specified and *P*-values are calculated using the log-rank test. **(b)** P-V and P- Δ N α were plated at the density of 100 cells/well in triplicate in six-well plates and after 2 weeks the colonies were stained with crystal violet. Colonies were counted and their morphology analyzed through light microscopy. Results are presented as mean \pm s.e.m. of three biological replicates.

At high density, there was no increase in apoptosis levels (Supplementary Figure 2A), possibly reflecting a function for Δ Np63 in survival at high density through reversible growth inhibition and acetylation.²⁰ Performing immunoprecipitation (IP) western blotting in PC3 cells grown at high density to enrich for possible low-level expression, we could detect Δ Np63 α protein. As a control, we used RWPE-1 cells, a non-transformed line enriched in basal/stem cells, with high levels of the Δ Np63 α (Figure 1b). Again, expression was not detectable in LNCaP or DU145.

Given that Δ Np63 α was present at such low levels in PC3, this suggested that expression might be low in every cell, or that only some cells might express detectable protein. To address this, we performed immunocytochemistry in culture. Remarkably, this identified that a sub-population of cells specifically expressed p63 in PC3 (Figure 1c) and not in the non-bone metastatic cell lines LNCaP and DU145 (Supplementary Figure 2B). However, as the PC3 line is derived from a bone metastatic tumor, we wanted to examine whether we could detect a similar pattern of p63 in bone metastatic prostate tumors *in vivo*. To achieve this, we performed intra-cardiac injections of the PC3 cell line, an assay to assess the potential homing and colonization to metastatic sites, as well as intra-tibial injections, which measures the ability of metastatic cells to adhere and grow within the bone microenvironment. These two models are particularly useful as there are no genetically engineered mouse models that spontaneously metastasize to the bone.^{21,22} Subsequently, the tumors that developed were stained for total p63 and Δ Np63. As is shown in Figure 1d, intra-tibial tumors in the bone were stained with H&E and

Masson's Trichrome to identify the location of the bone. Then immunostaining for p63 (all isoforms) and the Δ Np63 isoform showed that, in agreement with our *in vitro* data, individual p63- and Δ Np63-positive cells were detectable in the metastatic lesions that developed in the bone (Figure 1d and Supplementary Figure 2C). This surprising observation uncovers previously unknown heterogeneity in the PC3 cell line.

Δ Np63 α promotes colonization of prostate metastatic cells to the bone

Next, we investigated the effects of alteration of Δ Np63 expression on the PC3 cell line *in vivo*. First, we overexpressed Δ Np63 α in PC3 cells, along with a luciferase vector, and directly injected 250 000 cells into the tibia of nude mice to measure for effects on tumor growth in the bone (Figure 2a). Here the effects were striking, in that enhanced expression of Δ Np63 α in bone metastatic PC cells increased the early colonization and growth of the bone metastatic lesions *in vivo*. For example, at 3 weeks post-injection, 5/7 mice receiving control cells did not yet display any tumor-bearing luciferase signal, whereas 7/9 mice that had been injected with Δ Np63 α , already had detectable tumor growth (Figure 2a). This increased tumor intensity persisted throughout the course of the study, resulting in the Δ Np63 α -expressing mice having to be killed/dying sooner than controls (table inset, Figure 2a). These differences were less obvious however when higher numbers of cells (1×10^6) cells were injected (data not

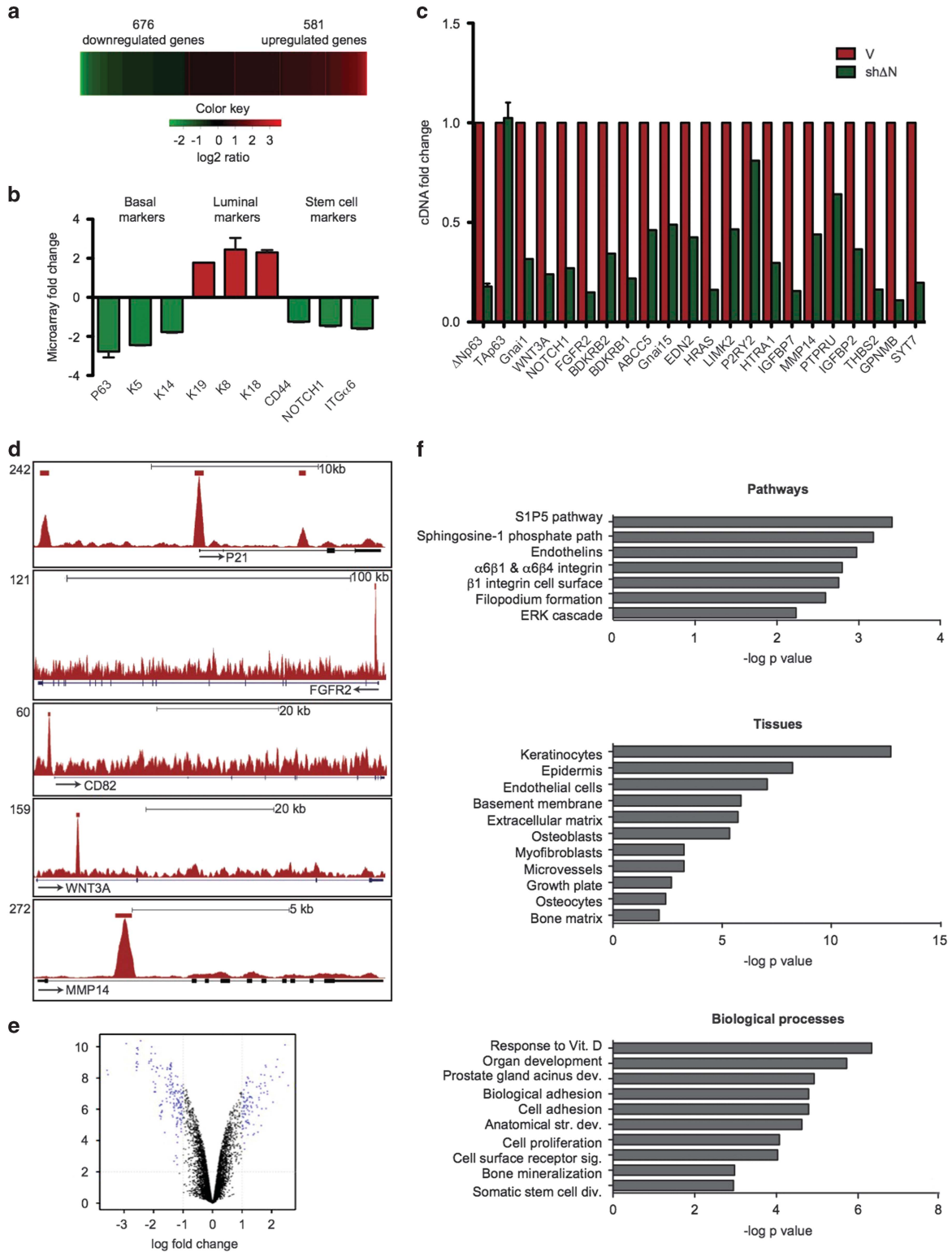


Figure 3. Δ Np63 directly regulates genes involved in epithelial development, stem cells and the bone microenvironment. **(a)** Microarray analysis of RWPE-1 cells infected with a short hairpin for Δ Np63 (R-sh Δ N) compared to RWPE-1 infected with vector control (R-V) was performed. The heat map represents the microarray results, with a fold change threshold of 1.4 and the P -value at 0.05. **(b)** Depiction of basal, luminal and stem cell genes that were up- and downregulated in R-sh Δ N, compared to R-V in the microarray. **(c)** RT-qPCR validation of some of the genes identified in the microarray. cDNA fold changes are compared to values in R-V. Two biological replicates are presented for Δ Np63 and TAp63, and one for the other genes. **(d)** ChIP-Seq analysis for p63 was performed in RWPE-1. Mapping peaks of p63 targets p21, FGFR2, WNT3A, BDKRB1 and MMP14 are shown. **(e)** Volcano plot of the common genes found in the microarray with Δ Np63 knockdown and ChIP-Seq. **(f)** Genomatix software analysis of direct p63-target genes downregulated in microarrays of R-sh Δ N compared to R-V showing the over-represented pathways, tissues and biological processes (full analysis and gene lists in Supplementary Table 2).

shown), further highlighting the role of p63 in early metastatic growth.

Interestingly, the PC3 cell line contains a population of holoclone cells that display cancer stem-like properties and that contribute to tumor growth and renewal (Doherty *et al.*¹¹, Li *et al.*¹², Zhang and Waxman¹³). Given that p63 is a key mediator of stem-like properties in normal prostate and other cancer types, we next asked whether increased expression of *ΔNp63a* had any effect on holoclone growth patterns in PC3 cells. Interestingly, upon overexpression of *ΔNp63a*, there was a significantly higher number of holoclones and fewer paraclones, supporting the idea that *ΔNp63a* might contribute to the stem-like properties in these cells (Figure 2b).

These findings suggest that an investigation of *ΔNp63a* in these cells might serve to uncover mechanistic links between stem-like properties and metastatic tumor growth. To address this, we first generated shRNAs specifically targeting the *ΔNp63* isoform, and validated their specificity in the non-transformed prostate cell line RWPE-1, that has basal stem-like characteristics (Supplementary Figure 3A). Interestingly, knockdown of *ΔNp63* in this cell line led to a decrease in growth ability as measured by growth curve and focus-formation assays (Supplementary Figures 3B,C). In addition, the RWPE-1 cell line, due to its stem-like properties, forms spheres in 3D culture. These features were also significantly impaired with knockdown of *ΔNp63*, resulting in fewer and smaller spheres at first and second passage, supporting a role for *ΔNp63a* in regulating adult PSC growth (Supplementary Figure 3D).

ΔNp63 directly controls expression of genes involved both in epithelial stem cell maintenance, bone survival and adhesion

As a first step to identify prostate-specific genes whose expression is regulated by *ΔNp63a*, we performed microarray analysis on the RWPE-1 cell line following knockdown of the *ΔN* isoform, which causes loss of stem-like proliferative capacity in these cells. We identified a total of 581 genes whose expression increased, and 676 genes whose expression decreased upon knockdown of *ΔNp63* (Figure 3a). Interestingly, loss of *ΔNp63* induced a downregulation of basal markers, and an increase in luminal markers (Figure 3b), as well as decreased expression of known stem cell genes, including WNT3A, CD44, ITGA6, NOTCH1 and FGFR2 (Figures 3b and c).

Next, we wanted to identify those genes that are direct transcriptional targets of p63 in prostate cells. While this has been done for keratinocytes, similar data for the prostate have not been generated. With this purpose, we performed chromatin-IP followed by high-throughput sequencing (ChIP-Seq) on RWPE-1 cells. Importantly, this identified a number of previously known targets of p63, including P21, PERP, CD82 and FGFR2, as well as new ones including WNT3A and MMP14 (Figure 3d). Then, by overlapping the complete list of p63 targets with our microarray data set, we could identify those p63-target genes whose expression was altered by loss of *ΔNp63*, and that might mediate the stem-like properties of p63 in the prostate (Figure 3e). As *ΔNp63a* can act both as a transcriptional repressor or an activator of gene expression, we were initially interested in identifying those p63 targets whose expression was activated by p63, so we focused on the downregulated list. Using the Genomatix software to perform Gene Ontology and Pathway analysis, we identified interesting signatures (Figure 3f and Supplementary Table 1). As might be expected, in prostate cells, *ΔNp63* expression correlated with pathways relating to epithelial status and stem cell function. Surprisingly however, terms relating to bone were also identified, including 'osteoblasts', 'bone matrix' and 'osteocytes', suggesting that, even in basal stem-like cells, *ΔNp63a* mediates a set of genes that are related to bone survival and growth. Moreover, among the most prominent signatures detected were 'adhesion' and adhesion-related events including 'ECM' and 'basement

membrane', suggesting that *ΔNp63* might be regulating these properties in PSCs.

To determine whether *ΔNp63a* might be regulating similar processes in the metastatic cancer cell line, we performed microarray on PC3 cells in which *ΔNp63a* was overexpressed, and which exhibit increased bone metastasis *in vivo*. This identified a total of 43 upregulated and 19 downregulated genes (Figure 4a). Then finally, by comparing those lists of genes that exhibited a significant increase in PC3 cells upon *ΔNp63a* overexpression, with the list of direct p63-target genes that displayed significantly reduced expression upon knockdown of *ΔNp63a* in RWPE-1 cells, we were able to identify 11 genes in common, that are directly activated by *ΔNp63a* in normal PSCs and PC bone metastasis (Figures 4b and c). Remarkably, these genes could be classified into functional categories, including 'adhesion' and 'homing to the bone', as well as 'drug metabolism' and 'membrane transport'. Furthermore, those genes linked to adhesion and bone homing (CD82, ITGB4, IL1B and DST) have previously been linked with p63 expression in other settings,^{23–26} supporting the specificity of our findings in PC.

The p63-target CD82 mediates bone metastatic adhesion

Given that cellular adhesion emerged as a major molecular signature in our profiling studies, and the increasing link with p63 and adhesive function in different settings,^{27–29} we investigated if this might also be important in prostate bone metastatic cell behavior. First, we checked whether increased expression of *ΔNp63a* in PC3 cells might confer increased adhesive properties on different ECM substrata (Figure 4d). Importantly, overexpression of *ΔNp63a* caused a significant increase in adhesion in every condition tested, including fibronectin and laminin I (Figure 4d), as well as collagen I (not shown).

Of the adhesion-related genes identified in our analysis, CD82 (also known as KAI-1) is a well-known epithelial-mesenchymal transition (EMT) suppressor and has been linked with adhesion and homing of hematopoietic and leukemic stem cells to the bone microenvironment, prompting us to investigate it further.^{30–32} Interestingly, we found that PC3 cells contain a sub-population of CD82-positive cells, which, upon *ΔNp63a* overexpression was significantly increased (Figure 5a). Since CD82 expression was also only detected in some cells in a manner similar to *ΔNp63*, we investigated whether these might represent a similar sub-population in prostate metastatic cells. To address this, we purified the CD82-high cells from the PC3 population and examined for expression of the 11 *ΔNp63*-regulated genes (Figure 5b). Interestingly, many of these same genes were expressed at significantly higher levels in the CD82-high population, supporting the concept that CD82 might be a mediator of the adhesion and metastatic properties of *ΔNp63*.

To investigate this possibility, we obtained shRNAs targeting CD82, and tested if these hairpins could successfully disrupt expression at the transcript and protein level, in PC3 cells overexpressing *ΔNp63a* (Figure 5c). Next, using the two most effective shRNAs with high knockdown efficiency, we examined whether knockdown of CD82 might diminish the adhesion mediated by *ΔNp63a*. Indeed, in PC3 cells overexpressing *ΔNp63a*, knockdown of CD82 with two separate hairpins abolished the adhesion of these cells, identifying this gene as a key player in *ΔNp63*-mediated adhesion (Figure 5d). To further investigate the possibility that targeted intervention with CD82-mediated signaling might affect *ΔNp63a*-driven adhesion, we treated the cells with an antibody to CD82 and found that interference with the protein also significantly reduced adhesion in culture (Figure 5e). Together, this suggests that CD82 might be a novel regulator of *ΔNp63a* function in PC3 cells.

However, the most important test was to identify whether loss of CD82 also functioned to disrupt *ΔNp63a*-driven bone

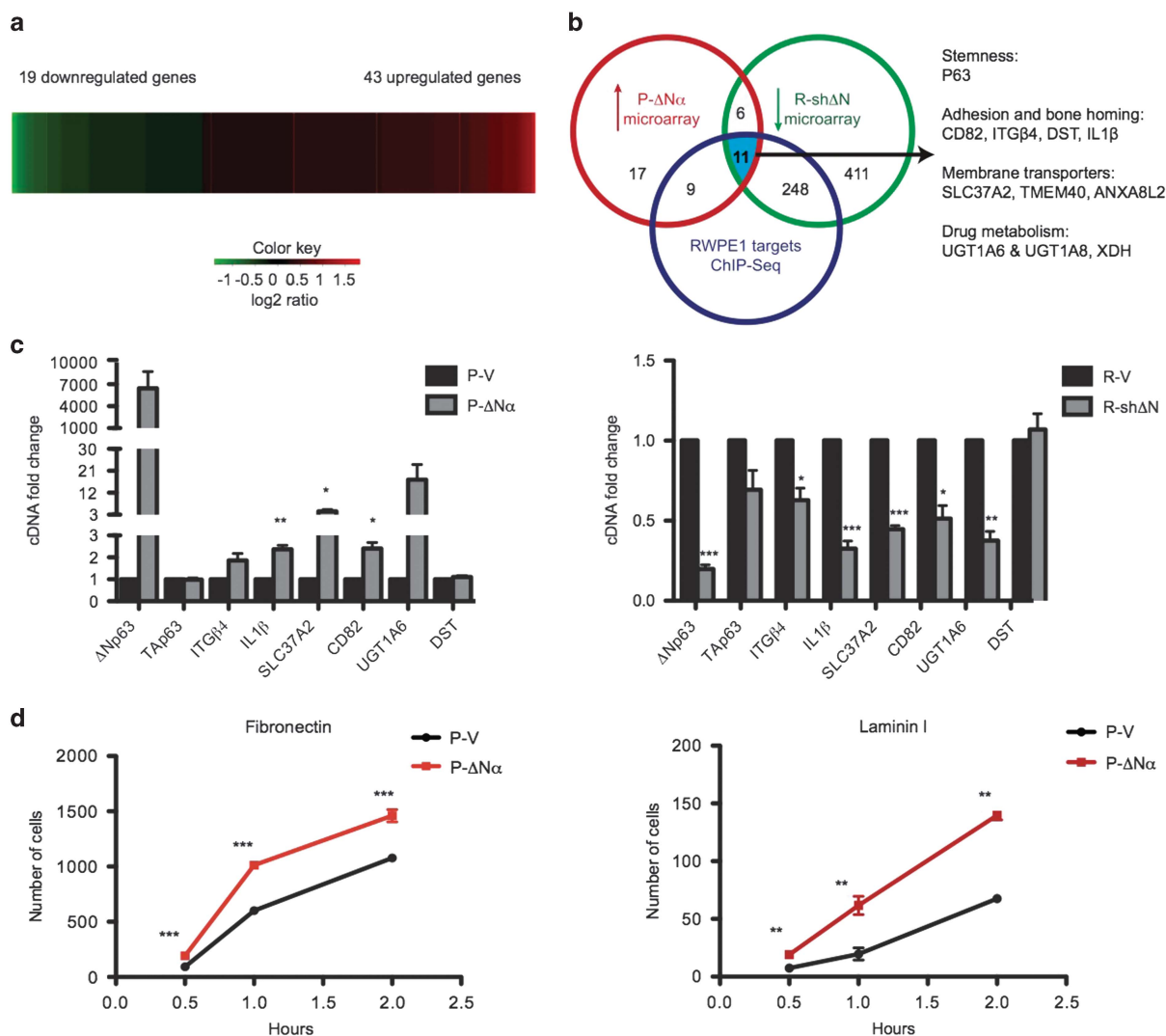


Figure 4. Δ Np63 directs a signature of genes favoring stemness and adhesion in prostate metastasis. **(a)** Microarray analysis was performed on P- Δ N α , compared to P-V. The heat map represents results setting the fold change threshold at 1.4 and the *P*-value at 0.05. **(b)** Representational comparison of genes upregulated by overexpression of Δ Np63 α in PC3, downregulated in RWPE-1 knocked down for Δ Np63 and that are direct targets of p63 identified by ChIP-Seq. **(c)** RT-qPCR for the validation of some direct targets of p63 changing accordingly with Δ Np63 both in PC3 and RWPE-1. Results presented as mean \pm s.e.m. from four and three biological replicates, respectively, for PC3 and RWPE-1. **(d)** P-V and P- Δ N α were plated on fibronectin- or laminin I-coated plates, and the number of cells adhering was counted. Results are presented as mean \pm s.e.m. of three technical replicates of one representative biological replicate of three attempts.

metastatic tumor growth *in vivo*. To address this, we again performed intra-tibial injections of the PC3- Δ Np63 α cells, this time with or without co-expression of the CD82 hairpin (Figure 5d). As before, PC3 cells with overexpression of Δ Np63 α formed large tumors that developed at early stages following injection. Remarkably however, in the absence of CD82, metastatic tumor growth was practically non-existent. Together, this demonstrates that CD82-mediated adhesion, regulated by Δ Np63 α , directly contributes to bone metastatic tumor colonization and growth, and suggests possible new avenues for therapeutic intervention.

CD82 mediates adhesion in other metastatic PC cells

These results uncovered previously unknown heterogeneity in the bone metastatic PC3 cell line, identifying a sub-population of cells that express Δ Np63 α , and which use CD82 to contribute to tumor cell adhesion and metastatic growth. This raises the question of whether these findings can provide information on broader mechanisms in epithelial tumor growth and metastasis. As

described previously,³³ CD82 has a wider expression in other PC metastatic cell lines (Figure 6a). To investigate if CD82 regulates a broader program of adhesion, we knocked down CD82 in these three main PC metastatic cell lines: PC3, DU145 and LNCaP (Figure 6b). Interestingly, knockdown of CD82 in each of the three cell lines led to changes in growth rates or proliferation, but the cells were still viable (Figure 6c). However, when subjected to adhesion assays, there was a clear and significant loss of adhesion in each cell type upon CD82 knockdown 5 (Figure 6d), suggesting that this protein may play previously unknown roles in promoting metastatic colonization.

DISCUSSION

PC is one of the main causes of cancer death of men in western countries, with metastasis to the bone representing the predominant incurable last step in the pathogenesis of the tumor. Indeed, the metastatic process is a complex multistep process, including EMT and invasion from the primary tumor,

dissemination through the blood and lymphatic vasculature, invasion into the metastatic organ, colonization and survival of the invading cells, culminating in the growth of the metastatic tumor.

In the absence of suitable genetic models to investigate this process in PC, many studies rely on the PC3 cell line, which exhibits metastasis to the bone (and other tissues) in a subset of

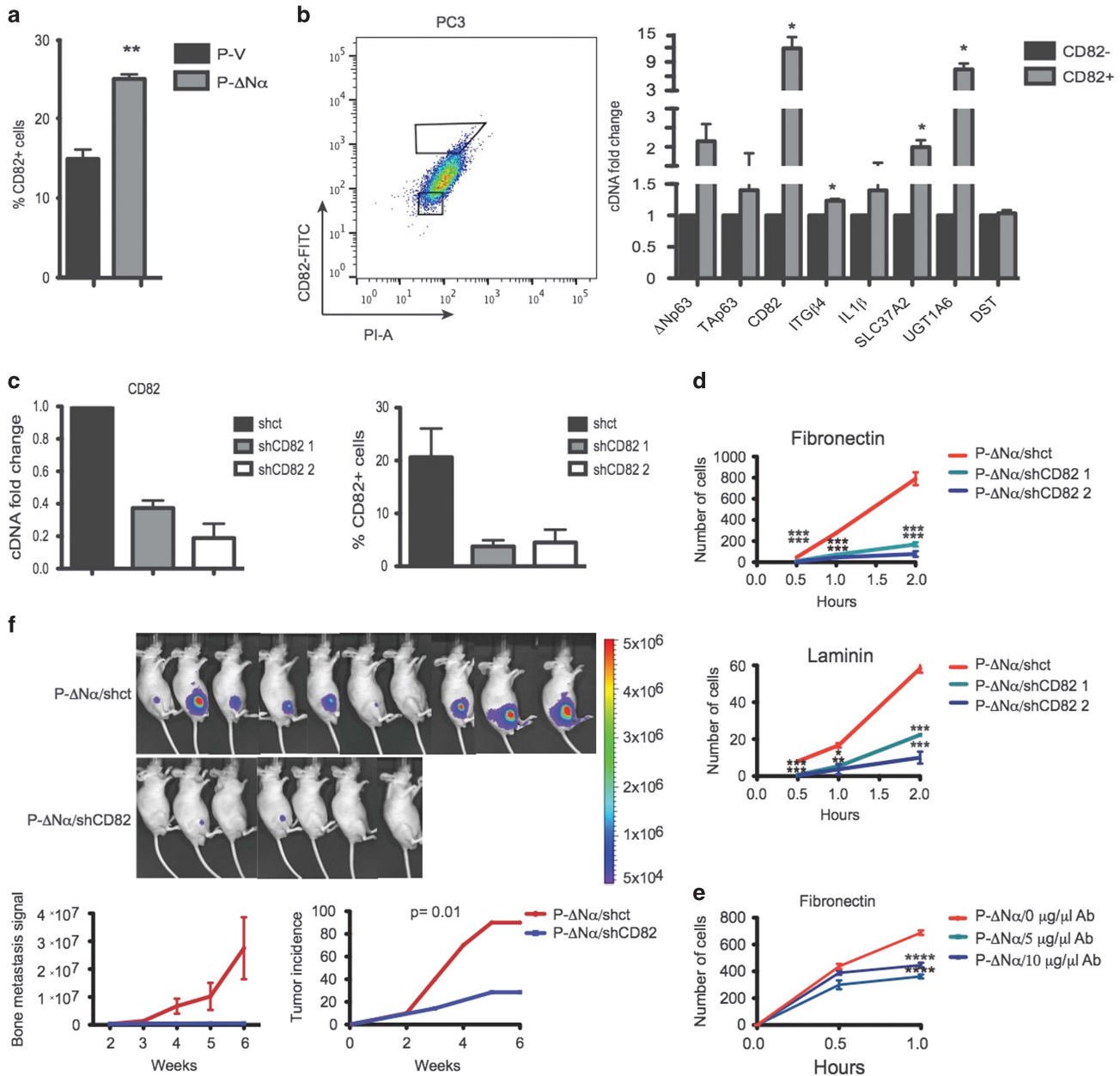


Figure 5. The p63-target CD82 controls metastatic adhesion mediated by Δ Np63 α *in vitro* and *in vivo* in the bone microenvironment. **(a)** PC3 cells infected with V or Δ Np63 α were stained for CD82 and analyzed by FACS. Representative FACS plot and graph showing the percentage of CD82+ cells as mean \pm s.e.m. of three biological replicates. **(b)** CD82+ and CD82- cells were sorted from PC3. Levels of the two isoforms of p63 and of other genes directly regulated by Δ Np63 were analyzed by RT-qPCR in the two populations. One representative FACS plot of three experiments is shown and graph depicts results as mean \pm s.e.m. from three biological replicates, with values compared to the PC3 CD82- population. **(c)** shRNAs targeting CD82 were infected into PC3 cells overexpressing Δ Np63 α . The efficiency of knockdown was tested by RT-qPCR (transcript) and FACS (protein). RT-qPCR values were compared to cells infected with a short hairpin control (shct) and results are presented as mean \pm s.e.m. of three biological replicates. Representative FACS plots depict one of three experiments. **(d)** P- Δ N α +shct, P- Δ N α +shCD82 1 and P- Δ N α +shCD82 2 were plated in the presence of fibronectin or laminin I. An adhesion assay was performed as previously described in Figure 4. Results are presented as mean \pm s.e.m. of three technical replicates of one representative biological replicate of two attempts. **(e)** P- Δ N α cells were treated with different concentrations of CD82-blocking antibody and plated in the presence of fibronectin. An adhesion assay was performed as previously described in Figure 4. Results are presented as mean \pm s.e.m. of three technical replicates of one biological replicate. **(f)** Adult male nude mice were injected intra-tibially with 2.5×10^5 P- Δ N α +shct+Luc-GFP and P- Δ N α +shCD82+Luc-GFP. Bone metastasis was monitored weekly by luciferase imaging starting from week 3. Ten mice were analyzed for the P- Δ N α +shct group and seven for the P- Δ N α +shCD82 group. Animals were killed at week 6. Imaging of mice at week 6 is shown and luciferase signal is represented as mean \pm s.e.m. The tumor incidence refers to the total number of mice developing lesions from the beginning of the study, *P*-values are calculated using the log-rank test.

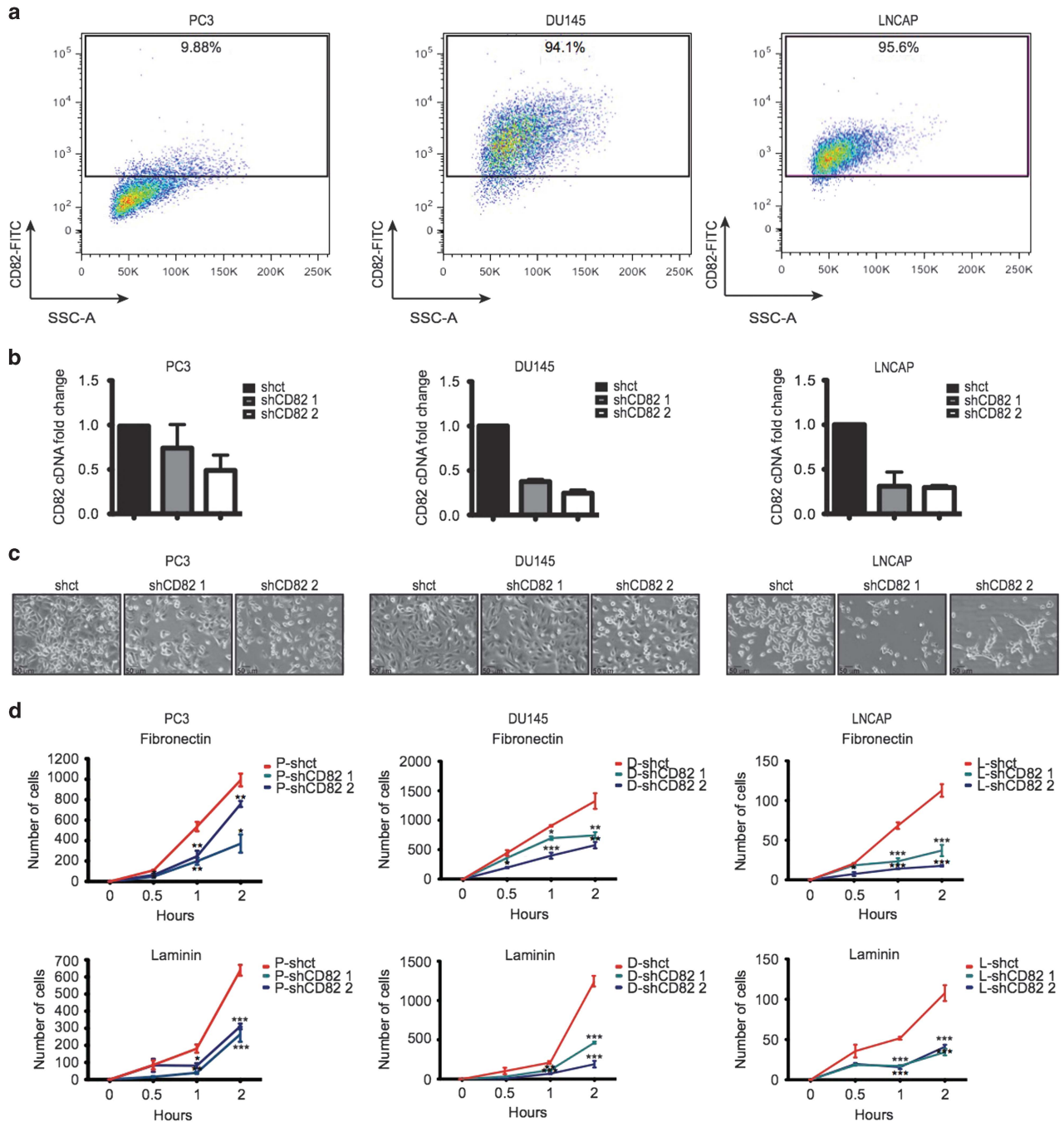


Figure 6. CD82 mediates adhesion also of non-bone metastatic PC cells. **(a)** FACS plots of PC3, DU145 and LNCaP stained for CD82. The percentage of positive cells is indicated. **(b)** The shRNAs targeting CD82 were infected into PC3, DU145 and LNCaP. RT-qPCR values were compared to cells infected with a short hairpin control (shct) and results are presented as mean \pm s.e.m. of two biological replicates. **(c)** Representative pictures of the three cell lines infected either with shct or the two shs for CD82 in culture. **(d)** PC3, DU145 and LNCaP infected with either shct or the two shs for CD82 were plated in the presence of fibronectin or laminin I. An adhesion assay was again performed as previously described in Figure 4. Results are presented as mean \pm s.e.m. of three technical replicates of one representative biological replicate of two attempts.

mice following intra-cardiac injection. Interestingly, this cell line also contains populations of cancer stem-like cells that favor clonal growth and tumor growth.^{11–13} Our results uncover a previously unknown sub-population of p63-positive cells in PC3, and identify a role for Δ Np63a in mediating prostate metastatic colonization to the bone and favoring the growth of the tumor in this microenvironment (Figure 7). Importantly, this seems to be through increased adhesion of tumor cells in the bone metastatic niche and the promotion of stem-like growth properties. The

concept that metastatic colonization involves stem-like events has previously been demonstrated in breast cancer,^{34–36} and our study now suggests similar mechanisms also function in PC.

Δ Np63a is a well-characterized mediator of stem cell function in a number of tissues, particularly during embryonic development.^{2,37} We demonstrate that it is the utilization of some of the same regulatory pathways and processes mediated by Δ Np63a in normal stem cells that favors bone metastatic tumor growth. These processes include adhesion of the colonizing cell,

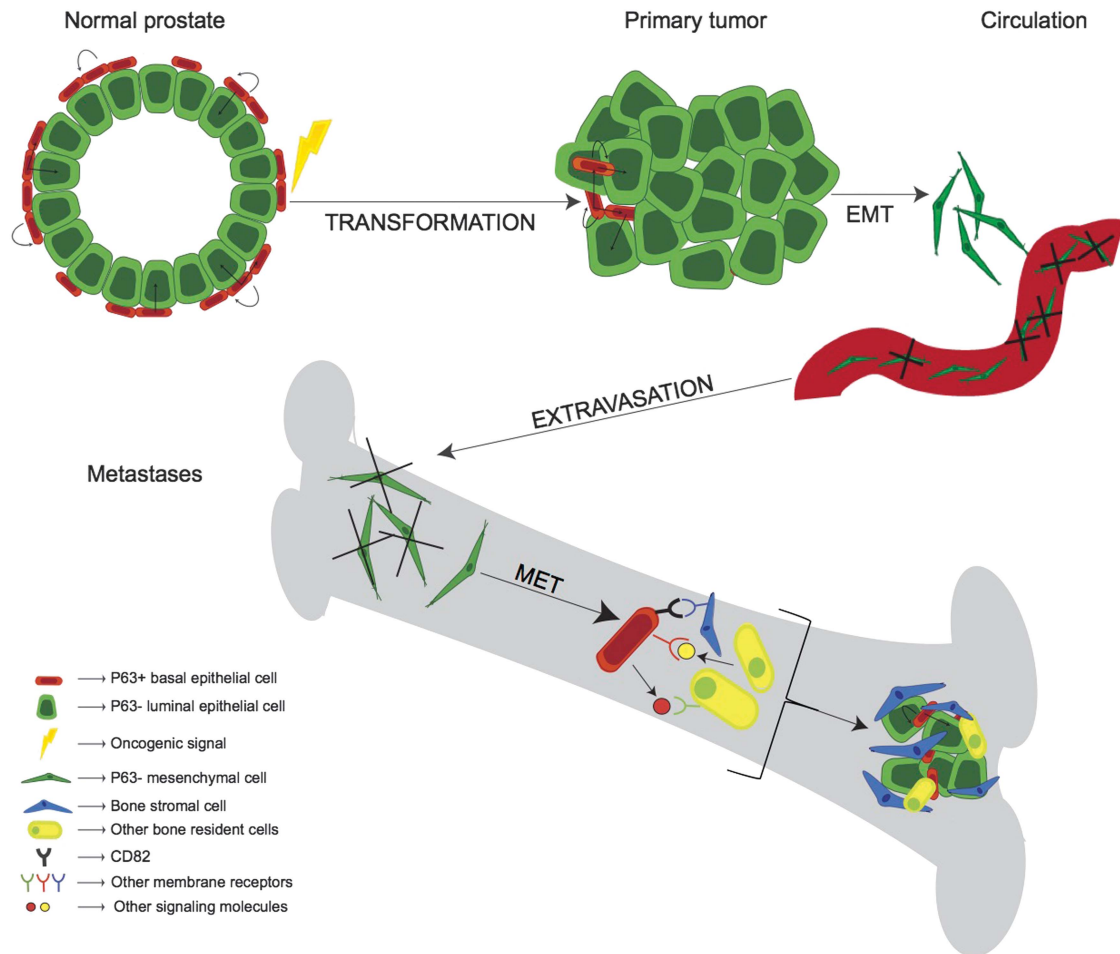


Figure 7. Model of p63 expression and function in PSCs and cancer. Δ Np63 α + basal PSCs give rise to Δ Np63 α - luminal differentiated cells and can be targeted for transformation generating mainly luminal cells that form the bulk of the primary tumor. Loss of Δ Np63 is necessary to undergo EMT, enter the circulation and invade distant sites. Few cells survive these processes and in PC, they predominantly colonize the bone where they re-acquire an epithelial/stem cell phenotype through mesenchymal-epithelial transition and colonize the new microenvironment. Our data suggest that this step requires reactivation of Δ Np63 α that drives the expression of molecules, such as CD82, necessary for adhesion to the bone. Δ Np63 α - cells could then derive from Δ Np63 α + colonizing cells and participate to the formation of the metastatic lesions together with stromal and other bone resident cells.

signaling to the local microenvironment to create a niche and the likely recruitment of cooperating cell populations. Intriguingly, the fact that some of the p63-regulated pathways that help maintain normal PSC growth facilitate survival in the bone microenvironment might help to explain the predominance of metastasis to the bone with these tumors.

Moreover, this discovery that Δ Np63 α is expressed in the bone metastatic cells and in the metastatic tumors, while being clinically absent from primary tumors, raises the possibility that the bone microenvironment might favor the re-expression of p63 at different stages of tumor progression. Interestingly, Δ Np63 α -positive cells have been suggested as the cell of origin for PC,^{6,7} while, loss of p63 expression is important for EMT and tumor invasion.^{7,17-19,27} In addition, its forced re-expression is sufficient to re-activate epithelial traits in a mesenchymal-epithelial transition-like process.^{19,38} Our findings support these observations, that reactivation of Δ Np63 α in a subset of metastatic cells at later stages of colonization might promote mesenchymal-epithelial transition and as we show, adhesion at bone metastatic sites (Figure 7). Indeed, our data adds to the growing body of work linking p63 with adhesion and tumor progression,²⁷⁻²⁹ and uncovers an unexpected role for this process in prostate bone metastatic tumor growth.

While the bone microenvironment may play a role in reactivation of p63, why there exists a small sub-population of p63-positive cells in this the PC3 cell line and not the others remains unknown. Here it may be related to the fact that these cells are androgen independent. In normal prostate, removal of androgen stimulation through castration causes regression of the prostate. However, this also causes an accumulation of p63-positive cells in the regressed gland, which are required for maintenance in the absence of hormone, and gland regrowth upon hormone restoration.^{39,40} It is tempting to speculate that this enrichment of p63 in the absence of hormone may be related to the expression of p63 in the PC3 cell line. Of course, while the DU145 line also is androgen independent, PC3 retains the expression of coactivators necessary to mediate a response to hormone that is not present in the DU145 line,⁴¹ suggesting there are additional difference with regards to androgen independence between the two lines.

In addition, we also identified CD82, a known p63-target gene²⁵ as being common to normal stem-like and metastatic prostate cells, and demonstrated that regulated interaction with the external environment through adhesion and adhesion-related signaling plays a significant role in regulating metastatic colonization.^{34-36,42} Previously, CD82 has been well characterized as a metastasis suppressor at early stages of tumor development,

a promoter of adhesion and a suppressor of EMT in a variety of primary tumors.^{30,32,43,44} This is in part through the regulation of integrin- α 4 stability,⁴³ which was also enriched in Δ Np63 α and CD82-high cells in the current study. However, our data suggest that CD82 can also act as a promoter of the later stages of metastasis, and specifically of metastatic colonization of the target tissue. Importantly, our findings suggest that targeted interruption of the protein might actually decrease metastatic burden. Interestingly, CD82 has previously been linked with hematopoietic and leukemic stem cell adhesion and homing.^{31,45,46} Our identification here of a sub-population of metastatic PC cells with stem-like properties and increased adhesion raises the interesting possibility that CD82 may also play a role in PC stem cell growth, as the adhesion properties conferred by CD82 were confirmed in the two other main cell line used to model PC metastasis, DU145 and LNCaP.

Altogether, the unexpected identification here of a sub-population of Δ Np63 and CD82-positive cells, whose disruption significantly perturbs the development of prostate metastatic tumor growth, further supports that targeting the interaction with the metastatic niche might represent a viable therapeutic opportunity at later stages of tumor progression.

MATERIALS AND METHODS

Animal studies

Male C57BL/6 and Swiss Nude mice of 6–10 weeks old (Charles Rivers Laboratories, Wilmington, MA, USA) were maintained at the Barcelona Biomedical Research Park, (PRBB), following the animal care standards of the institution that complies with European legislation on the care and use of animals. For intra-cardiac injections, 1×10^6 cells were resuspended in 100 μ l of phosphate-buffered saline (PBS) and injected into the left ventricle of nude mice. Luciferase signal was acquired after 30 min and mice without a systemic distribution of the signal were discarded. For intra-tibial injections, 2.5×10^5 cells were resuspended in 20 μ l of PBS and injected into the right tibias of nude mice. Left tibias were injected the same way with PBS as control. For imaging, 400 μ l of 5 mg/ml potassium luciferin (GOLDBIO Cat#LUK1G) were injected intraperitoneally in each animal and signal was acquired after 10 min with the *in vitro* imaging system (IVIS) (Perkin Elmer) platform. Images were analyzed with the Igor Pro Carbon software. Luciferase signal is represented as mean \pm s.e.m. The tumor incidence refers to the total number of mice developing lesions from the beginning of the study, *P*-values are calculated using the log-rank test.

ShRNA design and cloning

For shRNA design, http://gesteland.genetics.utah.edu/siRNA_scales/ and http://cancan.cshl.edu/RNAi_central/RNAi.cgi?type=shRNA were used. The oligonucleotides were purchased from Invitrogen (Carlsbad, CA, USA) and were cloned in the pLMP-GFP-Puro retroviral expression vector.⁴⁷ The sequence of the sh Δ Np63 used in our studies is 5'-TGCTGTTGACAGTGAGCGCAAGGACAGCAGCATTGATCAATAGTGAAGCCACAGATGTATTGATCAATGCTGCTGCTCTTTTGCTACTGCTCGGA-3'. For knockdown of CD82, five CD82 hairpins and a short hairpin control were purchased from Sigma-Aldrich (St Louis, MO, USA): TRCN0000245060, TRCN0000038029, TRCN000038030, TRCN0000038032, TRCN0000038033 and SHC002 in the pLKO.1-puro vector. For overexpression studies, the retroviral control vector pMSCV-GFP-Puro and pMSCV-GFP-Puro containing full-length mouse Δ Np63 α vectors were used.⁵ pMSCV-Luc-GFP-Neo was a gift from Johannes Zuber, IMP, Vienna.

Cell lines, viral production and infection

RWPE-1 cells were purchased from ATCC (Manassas, VA, USA). PC3, LNCaP and DU145 were a kind gift of Maria Paola Paronetto, Fondazione Santa Lucia, Università degli studi di Roma 'Foro Italico'. Phoenix packaging cells (G Nolan, Stanford University, Stanford, CA, USA) were used for retrovirus production following previously described transfection procedures.⁵

Focus-formation assay, colony-formation assay and 3D culture

For focus-formation assay, 2000, 4000 and 8000 cells were cultured in duplicate in six-well plates. At day 10, cells were fixed and stained with 0.5% crystal violet in 20% MetOH. For colony-formation assay, 100 cells were cultured in triplicate in six-well plates and at 2 weeks, the cells were fixed and stained as before. *P*-values were calculated on three biological replicates using unpaired *t*-test for the number of colonies and two-way Anova with Bonferroni post-test for the percentage of holoclones, meroclones and paraclones. 3D cultures were performed as previously described.^{48,49} 2.5×10^3 cells were seeded into eight-well chamber slides (BD Falcon, Corning, NY, USA). Values from five and three experiments, respectively, for P1 and P2, are combined for quantification of number and area of at least 200 spheres/8 fields of view per condition per experiment.

The imaging software ImageJ was used for analysis. Statistical significance was determined by two-tailed Student's *t*-test.

Adhesion assay

Forty-eight-well plates were coated with collagen I 1:100, fibronectin 20 μ g/ml, laminin I 10 μ g/ml (R&D systems, Minneapolis, MN, USA). Cells were plated at a concentration of 4×10^5 /ml in a volume of 250 μ l per well. At 30 min, 1 and 2 h after plating, adherent cells were fixed and attached cells were stained with 0.5% crystal violet in 20% MetOH for 10 min and counted with a $\times 40$ objective in five randomly chosen fields per three wells for each condition. Statistics were performed using one-way Anova and Tukey's multiple comparisons tests.

Flow cytometry

The antibodies for Sca-1 (FITC, E-13-161.7, BD Pharmigen, San Diego, CA, USA) and CD49f (PE, GoH3, BD Pharmigen) were used at a concentration of 1:100. CD82 was detected using the B-L2 antibody (Abcam, Cambridge, UK) and a secondary antibody conjugated with Alexa Fluor 488 or 568 (Invitrogen), respectively, 1:100 and 1:500. Cells were analyzed on the LSR Fortessa flow cytometer or sorted on the FACSaria cell sorter (BD Biosciences, San Diego, CA, USA) and data examined with FlowJo software (Tree Star, Ashland, OR, USA).

Cytospin

Prostates from 6–10-week-old wild-type C57BL/6 mice and were incubated in 5 mg/ml Dispase II (Roche, Basel, Switzerland) at 4 °C o/n. The tissue was minced and stirred for 30 min at RT. Dissociated cells were sorted and attached to a slide by spinning in a cytospin 4 centrifuge (Thermo Shandon, Cambridge, UK). For quantification after immunocytochemistry, cells were counted and statistics were performed using two-way Anova with Bonferroni post-test

Immunocytochemistry

Cells were washed, fixed and incubated 1 h at RT with blocking solution: PBS, 10% goat serum, 0.5% Tween 20 (Sigma-Aldrich). Primary and secondary antibodies were incubated, respectively, o/n at 4 °C and 1 h at RT. Primary antibody for p63 (4A4) was used at a concentration of 1:200. Secondary antibody conjugated with Alexa Fluor 568 (Invitrogen) was used 1:1000.

Histological sample processing, immunofluorescent and immunohistochemical stainings

Bones were fixed in 4% PFA o/n at 4 °C and decalcified in 10% EDTA at 4 °C for 3 weeks. All the samples were embedded in paraffin and sectioned. Antigen retrieval was performed by boiling the sections for 20 min in EDTA buffer and cooling to RT for 1 h.

For immunohistochemistry, sections were treated with 0.3% H₂O₂ in PBS for 15 min at RT. Permeabilization was performed with 0.2% Tween 20 (Sigma-Aldrich) for 5 min at RT and blocking solution (10% goat serum, 0.1% Tween 20 in PBS) was added for 1 h at RT. Primary and secondary antibodies were incubated, respectively, o/n at 4 °C and 1 h at RT. Antibodies for CK5 (H40, Santa Cruz Biotechnology, Dallas, TX, USA), CK18 (H-80, Santa Cruz Biotechnology) and Δ Np63 (p40 5–17, Millipore, Darmstadt, Germany) were used, respectively, at concentration 1:500, 1:100 and 1:1000.

For immunofluorescence, secondary antibodies conjugated with Alexa Fluor 488 or 568 (Invitrogen) were used 1:1000. For immunohistochemistry, biotin-coupled secondary antibody incubation and avidin-peroxidase

label were performed with the ABC Kit (Vectastain, Vector Labs, Burlingame, CA, USA) and reactions were developed with DAB substrate kit for peroxidase (Vector Laboratories, Burlingame, CA, USA) according to the manufacturer's instructions. Hematoxylin counterstain was used for nuclei.

RT-qPCR

Total RNA was isolated using TRIzol Reagent (Life Technologies) or the RNeasy Mini Kit (QIAGEN, Hilden, Germany). One microgram of RNA was reverse transcribed using the SuperScript III First-Strand kit from Invitrogen or the qScript cDNA SuperMix from Quanta, in a reaction volume of 20 μl (50 ng/μl), which was diluted 1:10 (5 ng/μl), with 2 μl of this dilution (10 ng) were used for qRT-PCR. qRT-PCR reactions were performed in triplicate using SYBR Green Master Mix and a Light Cycler 480 Instrument (Roche Life Science, Basel, Switzerland). All kits were used according to the manufacturers' instructions. Relative levels of expression were determined relative to the housekeeping gene β-actin. Primers are listed in Supplementary Table 2. Three biological replicates were done for each experiment, unless differently specified. Results are presented in graphs as mean ± s.e.m. Statistical significance was determined by one-sample t-test.

Western blot and IP

For IPs and western blots, cells were lysed in IP300 buffer, sonicated 15 s at 10% output using a Branson sonicator and centrifuged for 20 min at maximum speed. IPs for p63 were performed using 50 μl of Protein A Sepharose 4 Fast Flow (GE Healthcare, Little Chalfont, UK) and 5 μg of the antibody clone H-137 from Santa Cruz. Control IPs were performed similarly using normal mouse IgG sc-2025 (Santa Cruz Biotechnology). An aliquot of 0.5 mg of RWPE-1 lysate and 4 mg of PC3, LNCAP and DU145 protein lysates were used for IPs. Western blot membranes were stained for p63 (4A4) (Santa Cruz Biotechnology) at a concentration of 1:200 o/n at 4 °C. α-tubulin was used as loading control and detected with the DM1A antibody (Sigma-Aldrich) at a concentration of 1:5000 1 h at RT. Anti-mouse IgG (GE Healthcare) was used as secondary antibody at a concentration of 1:5000 1 h at RT.

Microarray analysis and ChIP

For microarray analysis on RWPE-1 cells with knockdown of ΔNp63, three and four technical replicates of R-V and R-shΔN group were analyzed, respectively. For PC3 cells, two technical replicates were analyzed for P-V and four for P-ΔNα. Total RNA was extracted with the RNeasy Mini Kit (QIAGEN) and 100 ng were labeled using Low Input Quick Amp Labeling kit v6.5 (Agilent Technologies, Santa Clara, CA, USA; 5190-2305) following the manufacturer's instructions.

Chromatin IP was performed on RWPE-1 cells adapting the protocol from Keyes *et al.*⁵ The 4A4 antibody for p63 (Santa Cruz, SC-8431) was used. Libraries were prepared using the NEBNext ChIP-Seq Library Prep Reagent Set for Illumina kit (ref. E62005) according to the manufacturer's protocols.

CONFLICT OF INTEREST

The authors declare no conflict of interest.

ACKNOWLEDGEMENTS

We thank Roger Gomis and Marc Guiu for help with tumor imaging analysis, Jason Doles for help in the short hairpin design and the CRG Bioinformatics facility for assistance with microarray and sequencing data analysis. VDG was supported by a fellowship from 'La Caixa', and MP with an F.P.I. fellowship from the Spanish Ministry. This work was funded by Grants SAF2010-18829 (WMK) and SAF2013-49082-P (WMK) from the Ministerio de Economía y Competitividad and a Marie Curie International Reintegration Grant PIRG5-GA-2009-248262 (WMK).

REFERENCES

- 1 Yang A, Kaghad M, Wang Y, Gillett E, Fleming MD, Dotsch V *et al.* p63, a p53 homologue at 3q27-29, encodes multiple products with transactivating, death-inducing, and dominant-negative activities. *Mol Cell* 1998; **2**: 305–316.
- 2 Crum CP, McKeon FD. p63 in epithelial survival, germ cell surveillance, and neoplasia. *Annu Rev Pathol* 2010; **5**: 349–371.
- 3 Graziano V, De Laurenzi V. Role of p63 in cancer development. *Biochim Biophys Acta* 2011; **1816**: 57–66.

- 4 Hibi K, Trink B, Patturajan M, Westra WH, Caballero OL, Hill DE *et al.* AIS is an oncogene amplified in squamous cell carcinoma. *Proc Natl Acad Sci USA* 2000; **97**: 5462–5467.
- 5 Keyes WM, Pecoraro M, Aranda V, Vernersson-Lindahl E, Li W, Vogel H *et al.* ΔNp63α is an oncogene that targets chromatin remodeler Lsh to drive skin stem cell proliferation and tumorigenesis. *Cell Stem Cell* 2011; **8**: 164–176.
- 6 Goldstein AS, Huang J, Guo C, Garraway IP, Witte ON. Identification of a cell of origin for human prostate cancer. *Science* 2010; **329**: 568–571.
- 7 Wang S, Garcia AJ, Wu M, Lawson DA, Witte ON, Wu H. Pten deletion leads to the expansion of a prostatic stem/progenitor cell subpopulation and tumor initiation. *Proc Natl Acad Sci USA* 2006; **103**: 1480–1485.
- 8 Di Como CJ, Urist MJ, Babayan I, Drobnjak M, Hedvat CV, Teruya-Feldstein J *et al.* p63 expression profiles in human normal and tumor tissues. *Clin Cancer Res* 2002; **8**: 494–501.
- 9 Grisanzio C, Signoretti S. p63 in prostate biology and pathology. *J Cell Biochem* 2008; **103**: 1354–1368.
- 10 Signoretti S, Waltregny D, Dilks J, Isaac B, Lin D, Garraway L *et al.* p63 is a prostate basal cell marker and is required for prostate development. *Am J Pathol* 2000; **157**: 1769–1775.
- 11 Doherty RE, Haywood-Small SL, Sisley K, Cross NA. Aldehyde dehydrogenase activity selects for the holoclone phenotype in prostate cancer cells. *Biochem Biophys Res Commun* 2011; **414**: 801–807.
- 12 Li H, Chen X, Calhoun-Davis T, Claypool K, Tang DG. PC3 human prostate carcinoma cell holoclones contain self-renewing tumor-initiating cells. *Cancer Res* 2008; **68**: 1820–1825.
- 13 Zhang K, Waxman DJ. PC3 prostate tumor-initiating cells with molecular profile FAM65Bhigh/MFI2low/LEF1low increase tumor angiogenesis. *Mol Cancer* 2010; **9**: 319.
- 14 Mills AA, Zheng B, Wang XJ, Vogel H, Roop DR, Bradley A. p63 is a p53 homologue required for limb and epidermal morphogenesis. *Nature* 1999; **398**: 708–713.
- 15 Signoretti S, Pires MM, Lindauer M, Horner JW, Grisanzio C, Dhar S *et al.* p63 regulates commitment to the prostate cell lineage. *Proc Natl Acad Sci USA* 2005; **102**: 11355–11360.
- 16 Yang A, Schweitzer R, Sun D, Kaghad M, Walker N, Bronson RT *et al.* p63 is essential for regenerative proliferation in limb, craniofacial and epithelial development. *Nature* 1999; **398**: 714–718.
- 17 Mulholland DJ, Xin L, Morim A, Lawson D, Witte O, Wu H. Lin-Sca-1+CD49high stem/progenitors are tumor-initiating cells in the Pten-null prostate cancer model. *Cancer Res* 2009; **69**: 8555–8562.
- 18 Lawson DA, Zong Y, Memarzadeh S, Xin L, Huang J, Witte ON. Basal epithelial stem cells are efficient targets for prostate cancer initiation. *Proc Natl Acad Sci USA* 2010; **107**: 2610–2615.
- 19 Tucci P, Agostini M, Grespi F, Markert EK, Terrinoni A, Vousden KH *et al.* Loss of p63 and its microRNA-205 target results in enhanced cell migration and metastasis in prostate cancer. *Proc Natl Acad Sci USA* 2012; **109**: 15312–15317.
- 20 Chae YS, Kim H, Kim D, Lee H, Lee HO. Cell density-dependent acetylation of ΔNp63α is associated with p53-dependent cell cycle arrest. *FEBS Lett* 2012; **586**: 1128–1134.
- 21 Park SI, Kim SJ, McCauley LK, Gallick GE. Pre-clinical mouse models of human prostate cancer and their utility in drug discovery. *Curr Protoc Pharmacol* 2010; Chapter 14: Unit 14. 15.
- 22 Valkenburg KC, Williams BO. Mouse models of prostate cancer. *Prostate Cancer* 2011; **2011**: 895238.
- 23 Liu Q, Russell MR, Shahriari K, Jernigan DL, Lioni MI, Garcia FU *et al.* Interleukin-1β promotes skeletal colonization and progression of metastatic prostate cancer cells with neuroendocrine features. *Cancer Res* 2013; **73**: 3297–3305.
- 24 Osada M, Nagakawa Y, Park HL, Yamashita K, Wu G, Kim MS *et al.* p63-specific activation of the BPAG-1e promoter. *J Invest Dermatol* 2005; **125**: 52–60.
- 25 Wu J, Liang S, Bergholz J, He H, Walsh EM, Zhang Y *et al.* ΔNp63α activates CD82 metastasis suppressor to inhibit cancer cell invasion. *Cell Death Dis* 2014; **5**: e1280.
- 26 Wu N, Rollin J, Masse I, Lamartine J, Gidrol X. p63 regulates human keratinocyte proliferation via MYC-regulated gene network and differentiation commitment through cell adhesion-related gene network. *J Biol Chem* 2012; **287**: 5627–5638.
- 27 Barbieri CE, Tang LJ, Brown KA, Pietenpol JA. Loss of p63 leads to increased cell migration and up-regulation of genes involved in invasion and metastasis. *Cancer Res* 2006; **66**: 7589–7597.
- 28 Carroll DK, Carroll JS, Leong CO, Cheng F, Brown M, Mills AA *et al.* p63 regulates an adhesion programme and cell survival in epithelial cells. *Nat Cell Biol* 2006; **8**: 551–561.
- 29 Ferone G, Mollo MR, Missero C. Epidermal cell junctions and their regulation by p63 in health and disease. *Cell Tissue Res* 2015; **360**: 513–528.
- 30 Dong JT, Lamb PW, Rinker-Schaeffer CW, Vukanovic J, Ichikawa T, Isaacs JT *et al.* KAI1, a metastasis suppressor gene for prostate cancer on human chromosome 11p11.2. *Science* 1995; **268**: 884–886.

- 31 Nishioka C, Ikezoe T, Furihata M, Yang J, Serada S, Naka T *et al*. CD34(+)/CD38(−) acute myelogenous leukemia cells aberrantly express CD82 which regulates adhesion and survival of leukemia stem cells. *Int J Cancer* 2013; **132**: 2006–2019.
- 32 Tsai YC, Weissman AM. Dissecting the diverse functions of the metastasis suppressor CD82/KAI1. *FEBS Lett* 2011; **585**: 3166–3173.
- 33 Lee HA, Park I, Byun HJ, Jeoung D, Kim YM, Lee H. Metastasis suppressor KAI1/CD82 attenuates the matrix adhesion of human prostate cancer cells by suppressing fibronectin expression and beta1 integrin activation. *Cell Physiol Biochem* 2011; **27**: 575–586.
- 34 Gupta GP, Perk J, Acharyya S, de Candia P, Mittal V, Todorova-Manova K *et al*. ID genes mediate tumor reinitiation during breast cancer lung metastasis. *Proc Natl Acad Sci USA* 2007; **104**: 19506–19511.
- 35 Malanchi I, Santamaria-Martinez A, Susanto E, Peng H, Lehr HA, Delaloye JF *et al*. Interactions between cancer stem cells and their niche govern metastatic colonization. *Nature* 2012; **481**: 85–89.
- 36 Oskarsson T, Acharyya S, Zhang XH, Vanharanta S, Tavazoie SF, Morris PG *et al*. Breast cancer cells produce tenascin C as a metastatic niche component to colonize the lungs. *Nat Med* 2011; **17**: 867–874.
- 37 Senoo M, Pinto F, Crum CP, McKeon F. p63 is essential for the proliferative potential of stem cells in stratified epithelia. *Cell* 2007; **129**: 523–536.
- 38 Olsen JR, Oyan AM, Rostad K, Hellem MR, Liu J, Li L *et al*. p63 attenuates epithelial to mesenchymal potential in an experimental prostate cell model. *PLoS One* 2013; **8**: e62547.
- 39 Kurita T, Medina RT, Mills AA, Cunha GR. Role of p63 and basal cells in the prostate. *Development* 2004; **131**: 4955–4964.
- 40 Tien JC, Liu Z, Liao L, Wang F, Xu Y, Wu YL *et al*. The steroid receptor coactivator-3 is required for the development of castration-resistant prostate cancer. *Cancer Res* 2013; **73**: 3997–4008.
- 41 Litvinov IV, Antony L, Dalrymple SL, Becker R, Cheng L, Isaacs JT. PC3, but not DU145, human prostate cancer cells retain the coregulators required for tumor suppressor ability of androgen receptor. *Prostate* 2006; **66**: 1329–1338.
- 42 Seguin L, Desgrosellier JS, Weis SM, Cheresh DA. Integrins and cancer: regulators of cancer stemness, metastasis, and drug resistance. *Trends Cell Biol* 2015; **25**: 234–240.
- 43 Termini CM, Cotter ML, Marjon KD, Buranda T, Lidke KA, Gillette JM. The membrane scaffold CD82 regulates cell adhesion by altering α4 integrin stability and molecular density. *Mol Biol Cell* 2014; **25**: 1560–1573.
- 44 Tonoli H, Barrett JC. CD82 metastasis suppressor gene: a potential target for new therapeutics? *Trends Mol Med* 2005; **11**: 563–570.
- 45 Burchert A, Notter M, Dietrich Menssen H, Schwartz S, Knauf W, Neubauer A *et al*. CD82 (KAI1), a member of the tetraspan family, is expressed on early haemopoietic progenitor cells and up-regulated in distinct human leukaemias. *Br J Haematol* 1999; **107**: 494–504.
- 46 Larochelle A, Gillette JM, Desmond R, Ichwan B, Cantilena A, Cerf A *et al*. Bone marrow homing and engraftment of human hematopoietic stem and progenitor cells is mediated by a polarized membrane domain. *Blood* 2012; **119**: 1848–1855.
- 47 Dickins RA, Hemann MT, Zilfou JT, Simpson DR, Ibarra I, Hannon GJ *et al*. Probing tumor phenotypes using stable and regulated synthetic microRNA precursors. *Nat Genet* 2005; **37**: 1289–1295.
- 48 Aranda V, Haire T, Nolan ME, Calarco JP, Rosenberg AZ, Fawcett JP *et al*. Par6-aPKC uncouples ErbB2 induced disruption of polarized epithelial organization from proliferation control. *Nat Cell Biol* 2006; **8**: 1235–1245.
- 49 Harma V, Virtanen J, Makela R, Happonen A, Mpindi JP, Knuutila M *et al*. A comprehensive panel of three-dimensional models for studies of prostate cancer growth, invasion and drug responses. *PLoS One* 2010; **5**: e10431.



This work is licensed under a Creative Commons Attribution-NonCommercial-NoDerivs 4.0 International License. The images or other third party material in this article are included in the article's Creative Commons license, unless indicated otherwise in the credit line; if the material is not included under the Creative Commons license, users will need to obtain permission from the license holder to reproduce the material. To view a copy of this license, visit <http://creativecommons.org/licenses/by-nc-nd/4.0/>

© The Author(s) 2017

Supplementary Information accompanies this paper on the Oncogene website (<http://www.nature.com/onc>)